

Article

Not peer-reviewed version

---

# Evaluation of the Ability of Using Shear-horizontal Surface Acoustic Wave Biosensors to Perform Sterility Testing of Nutrient Media

---

[Aimofumhe Eshibomhe Sigmus](#)<sup>\*</sup>, Favour Badewole, Dy'Mond Smith, [Marlon Sheldon Thomas](#)<sup>\*</sup>

Posted Date: 1 March 2024

doi: 10.20944/preprints202403.0071.v1

Keywords: Shear-horizontal Surface Acoustic Wave (SH-SAW); Biosensor; Sterility testing; Escherichia coli K-12; Phase shift



Preprints.org is a free multidiscipline platform providing preprint service that is dedicated to making early versions of research outputs permanently available and citable. Preprints posted at Preprints.org appear in Web of Science, Crossref, Google Scholar, Scilit, Europe PMC.

Copyright: This is an open access article distributed under the Creative Commons Attribution License which permits unrestricted use, distribution, and reproduction in any medium, provided the original work is properly cited.

Article

# Evaluation of the Ability of Using Shear-Horizontal Surface Acoustic Wave Biosensors to Perform Sterility Testing of Nutrient Media

Aimofumhe Eshibomhe Sigmus, Favour Badewole, Dy'Mond Smith and Marlon Sheldon Thomas

Department of Life and Physical Sciences in the College of Natural Sciences and Mathematics, Fisk University, Nashville, Tennessee, 37208, USA

**Abstracts:** In this article, we describe a simple procedure for evaluating the sterility of nutrient media using a shear-horizontal surface acoustic wave (SH-SAW) biosensor. We used the SH-SAW biosensor platform to monitor the time-dependent phase responses of the material for the media that binds to a monolayer of 3-mercaptopropanyl-N-hydroxy succinimide on the biosensor surface. Increases in the phase shift less than 50% of the starting phase shift recorded 180 minutes after the sterilization indicate a successful sterility test of the media. Our devices were then applied to sterility testing using a viable *Escherichia coli* (*E. coli*) K-12 solution to confirm our hypothesis. Filtered LB Broth was the negative control, and a 24-hour culture of *E. coli* was the positive control. Before testing, the cell solution was pelleted, the media decanted and then replaced with a 1x phosphate-buffered saline solution (1x PBS). Since we know that the N-hydroxysuccinimide residues will bind to amine groups, only in cases where microbial species are present will the surface binding increase greater than 50%. We confirmed our hypothesis using SH-SAW biosensors and overnight *E. coli* cultures. The sensitivity for our 250 MHz quartz SH-SAW sensors was calculated based on the response from the *E. coli* K-12 solution over the linear dynamic range, which appears to be  $2 \times 10^4$ – $2 \times 10^7$  CFU per ml and has a sensitivity of  $S = 1.655 \times 10^5 \text{ }^\circ \text{m}^2 \text{ Kg}^{-1}$ . The limit of detection (LOD) for these sensors was calculated to be approximately  $2 \times 10^{-9}$  grams (g) which is estimated to be approximately 2,000 *Escherichia coli* (*E. coli*) K-12 cells. However, the sensitivity and insertion loss remained approximately unchanged before and after coating the sensor with 3,3'-Dithiobis(succinimidyl) Propionate (DSP).

**Keywords:** Shear-horizontal Surface Acoustic Wave (SH-SAW); Biosensor; Sterility testing; *Escherichia coli* K-12; Phase shift

## 1. Introduction

Shear-horizontal surface acoustic wave sensors are widely used in several industries, including the aerospace, automotive, and telecommunication industries. However, relatively little work has been done on establishing surface acoustic wave devices for use as point-of-care (POC) medical diagnostic tools.[1] Recent reports indicate that these devices are ideally suited for this role due to their small size, high sensitivities, and portability.[2,3] In particular, the guided shear-horizontal surface acoustic wave (SH-SAW) biosensors enable liquid phase measurements, a critical need for biomedical applications.[4,5] While lateral flow assays (LFAs) are considered the most prevalent POC devices due to their relatively low cost and their application for pregnancy testing.[7] These devices use a piece of treated paper called a nitrocellulose membrane to immobilize biological macromolecules such as a monoclonal antibody to rapidly indicate the presence of known amounts of antigens or antibodies to a surface that specifically targets biomarkers, pathogens, metabolites, or other antigens. SH-SAW devices have some inherent advantages to LFAs because they are electronic and can quantitatively measure concentration dependence in immunoassays.[7] Their electronic readouts are also easier to interpret than LFAs.[8] For these reasons, SH-SAW devices have attracted

significant attention as a real-time, label-free alternative to LPAs but can perform gas and liquid phase detection. [9]

Previously, we reported that we have developed SH-SAW methods to evaluate high-viscosity liquids and count red blood cells.[7,10] There have been others who have explored similar methods. Hsu-Chao Hao et al. demonstrated the ability to use an SH-SAW sensor coupled to a microfluidic device to capture eukaryotic cells using custom-built SH-SAW devices.[11] Thorsten N. Klauke et al. used commercially available surface acoustic wave devices from SAW Instruments, Germany, to target haptoglobin in porcine meat juice.[12] Chenyun Wang et al. used a similar commercially available device from the same, SAW Instruments, Germany, to quantitatively detect exosomes from human blood using mass enhancement from gold nanoparticles (AuNPs).[13] That SAW device was capable of detecting  $1.1 \times 10^3$  particles  $\text{ml}^{-1}$ , making it potentially suited for liquid biopsies.[13] Onur Tigli et al. and colleagues previously reported they developed a customized complementary metal-oxide semiconductor (CMOS) - SAW biosensor that was applied to cancer biomarker detection.[14] Youn-Suk Choi et al. and colleagues from the Samsung Advance Institute of Technology, demonstrate the detection of a series of cardiac biomarkers including cardiac troponin, creatine kinase, and myoglobin on a smaller, portable SAW biosensor within twelve minutes.[15] The device was modified and explored for use to detect bacterial cells. There have been a few other groups that have previously reported microbial species detection using surface acoustic wave devices. Marco Bisoffi et al. reported the detection of HIV I and HIV II using an SH-SAW biosensor.[16] Valerian Turbe and colleagues also reported HIV detection using a SH-SAW biosensor.[4,17] Junwang Ji et al. report the detection of *Pseudomonas aeruginosa* using a lithium tantalate SH-SAW biosensor.[18] Berkenpas et al. used an antibody-coated langasite surface acoustic wave sensor to detect *E. coli* in a dip and drip method.[19] We have also reported that SH-SAW biosensors can be made from different materials to minimize the effects of temperature or enhance sensitivity effects.[20] Due to our sensor's unique design, when analyzing liquid samples, we have built-in protection for reducing attenuation of the propagating acoustic wave.[17,21–23] We modified the existing gold-coated sensor by first coating the surface with the linker 3,3'-Dithiobis(succinimidyl) Propionate (DSP). DSP reduces to 3-mercaptopropanyl-N-hydroxysuccinimide ester with the addition of a reducing agent like tris (2-carboxyethyl) phosphine (TCEP).

In this paper, we used an SH-SAW biosensor to monitor the sterility of nutrient media after steam sterilization using a commercially available canner. The paper also reports the sensitivity of the SH-SAW biosensor to different solutions with different concentrations of *E. coli* K-12. Media sterilized with a low-cost canner was evaluated for microbial growth over a time course ranging from one minute after sterilization to 180 minutes after sterilization. A sample of Lysogeny broth (LB Broth) was sterilized and evaluated over the 180-minute time course. [24–29] Additionally, a second sample was developed and inoculated with *E. coli* K-12 immediately after sterilization. In this report, we successfully demonstrated an alternative quantitative approach by measuring the changes in bacterial species concentration on an SH-SAW biosensor. The sensors also demonstrated media sterility with less than 50% change in the phase shifts. The measured phase shift in the signals was directly correlated to the cell counts, as described previously and by other groups.

## 2. Material and Methods

*Escherichia coli* (*E. coli*) K-12 was purchased from Fisher Scientific; 3,3'-Dithiobis (succinimidyl) Propionate (DSP) was purchased from Fisher Scientific, 10x Phosphate buffered saline (PBS) was purchased from Fisher Scientific; Ultrapure water from Fisher Scientific, Saint Louis, MO; Tryptone; Yeast extracts; Sodium chloride; 200-proof ethanol; SYTO 11 red fluorescent dye (5  $\mu\text{M}$  in DMSO) was purchased from Life Technologies; Taiwan, and electronics from TST Biomedical Electronics; Gold-coated SH-SAW sensors from the TST Biomedical, Tris (2-carboxyethyl)phosphine (TCEP) purchased from Fisher Scientific; 1x PBS solution; LB Broth; Zeiss Axioskop 2 Plus, which is equipped with a Teledyne Lumenera INFINITY5-5 microscopy camera.

### 2.1. Experimental

A gold-coated quartz SH-SAW biosensor, having a central frequency centered at 250 MHz, was purchased from TST Biomedical Electronics Company and used without further modifications. The SH-SAW sensor has a corresponding phase velocity of  $v_0$  that Eqn describes. 1 below:

$$v_0 = f_0 \lambda \quad (1)$$

The acoustic wavelength of a quartz sensor with a center frequency of 250 MHz is approximately 20 microns. The SH-SAW biosensors used were all fabricated from quartz.[30] Although quartz has lower electro-mechanical coupling than some sensors made from other materials, such as lithium niobite and lithium tantalate, quartz has the unique advantage of having a near-zero temperature coefficient. [31] Therefore, quartz biosensors are not affected as severely by thermal drift and high coefficients of variances [30]. Therefore, these devices can be used without significant insulation around them or without having to use thermal compensation to correct the data. The SH-SAW sensors are coated with a 100 nm thin film of gold. The gold layer on the sensor plays several different roles, including shielding the sensor from interference from other devices, protecting the sensor from harsh chemicals, and enabling chemical functionalization of the sensor via gold-thiol chemistry [5]. The integrated transducers (IDTs) were designed to be excited with a single IDT with a reflector that exited and captured all signals from acoustic pulses and RF signals from the customized SH-SAW sensor. Each of the IDTs has a wavelength  $\lambda$  and a delay [4]. Each delay line was identical and encircled by a wall of the photoresist polymer, Su-8 [5]. The Su-8 well allows 5  $\mu$ l of the sample to be incubated [30]. The signal collected was the endpoint measurement which could be established in only 90 seconds since the sensors were incubated for 30 minutes with the *E. coli* K-12 solutions.



**Figure 1.** SH-SAW Biosensor System and gold-coated biosensor from TST Biomedical Electronics, (Taiwan). The sample reservoir is the black circle that surrounds the gold area that is visible in the middle of the biosensor.

## 2.2. Preparation of the SH-SAW Sensor

The uncoated SH-SAW sensors were cleaned sequentially by rinsing them with distilled water and then blowing them dry with compressed nitrogen. The sensors were then cleaned in a plasma cleaner for 90 seconds and then coated with 3% DSP in ethanol. A serial dilution of cell solutions was prepared with a 10x dilution series from  $2 \times 10^9$  colony-forming units per ml (CFU ml<sup>-1</sup>) over five decades. The insertion loss of the DSP-coated sensors was on average  $28.16 \pm 0.21$  dBm with an average phase shift (relative to the uncoated sensors) of  $13.1 \pm 4.8^\circ$ . Therefore, will look to see if signals of approximately  $20^\circ$  or higher will confirm failed sterility. We started each experiment by adding 5  $\mu$ l of distilled water to the sensor sample reservoir and recorded the phase response. Then, the water is removed from the sample reservoir and blown dry. The sample is then added to the reservoir while the phase response is recorded. The 1x PBS (without cells) reference signal is subtracted from the signal associated with the bacterial samples. The differences between the two samples represent phase shifts associated with the percent glycerol in each binary solution. The maximum signal, which was also used as the positive control was the 24-hour culture of *E. coli* K-12 in LB Broth, pelleted via centrifugation and re-suspended in 1x PBS buffer.

The dual-channel SH-SAW sensor was first coated with three percent DSP while submerged in ethanol. The *E. coli* samples were then diluted over five decades and used to coat sensors in quadruplets for each *E. coli* concentration. The sensor was assembled into the sensor and turned on. The baseline measurement is taken, the sample is added, and the sample is remeasured. The reference channel is used to account for any changes in environmental conditions. The difference in the sample and baseline signals gives the absolute signal.

The acoustic signal is transmitted via an interdigitated transducer (IDT) that both transmits and receives the signals after it travels across a delay line and then gets reflected by a reflector positioned at the end of the distal end of the sensor. This approach of using a sensor that has a single interdigitated transducer (IDT) reduces errors because all measures are made from a single transducer and it reduces the size of the sensor itself since the reflector doubles the transit time for the acoustic wave over the sample. The sensor can therefore be half the size of the dual sensors allowing you to measure the time it takes for the signal to transverse the delay line and the attenuation in the amplitude of the acoustic wave. The center frequency for the wave produced by the IDT is centered at 250 MHz. The sensor is fabricated on a 36° Y-cut quartz substrate. The device also features unique air cavities that cover the IDTs with a glass cover, and the cavity fills the case with air. The side walls are made from the epoxy photoresist Su-8 and sourced from MicroChem Corporation. The IDT is covered with a proprietary glass enclosure that protects the electrical contacts. The SH-SAW device was then assembled onto a printed circuit board (PCB) and wire bonded to the PCB.

We created a 10x dilution series from the *E. coli* K-12 stock solution in 1x PBS. The solutions were created and used to evaluate the phase responses to changes in the viscoelastic properties on the surface due to bacterial surface density changes. The bacterial solutions were pipetted into the 5  $\mu$ l sample reservoir and incubated for 30 minutes. The images of the *E. coli* K-12 cells were taken on a Zeiss Axioskop 2 Plus, which is equipped with a Teledyne Lumenera INFINITY5-5 monochrome microscopy camera. are seen in the SH-SAW sensor which is seen in Figure 3 (a) on a DSP-coated sensor plus fluorescent *E. coli* K-12 cell solution and (b) the sensor without any cells (negative control). The responses of the bacterial solution were similar to the phase shift of diluted solutions of varying dilutions of binary Glycerol-water solutions.

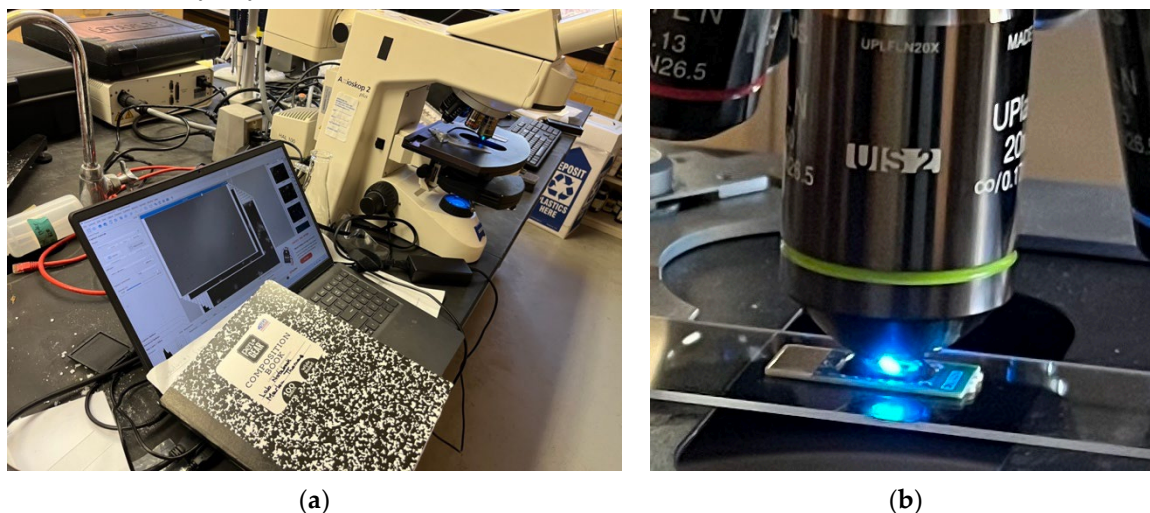


**Figure 2.** Photograph of the (a) SH-SAW electronic reader with sensor fluorescent imaging (b) photograph of the gold-coated SH-SAW biosensors with *E. coli* immobilized.

### 2.3. SH-SAW Electric reader

The electronic reader for the SH-SAW sensors is a dedicated electrical reader that interfaces with the sensor using a plug-in style connector. The connector is quite robust and ensures that there is always a stable connection between the reader and the sensor. The fluorescence exposure time is set using the fluorescence from the Su-8 material that forms the outer walls of the sample well.

The rate of propagation of SH-SAW across the gold-coated can be affected by the mechanical properties of the liquid. As a result, great attention must be paid to measurements in the attenuation of the SH-SAW signal with and without a thin film. We must coat the sensor with a capture agent, particularly when studying microbial species. The isolation and identification of bacterial pathogens often start with the non-selective capture of bacterial species on a semi-solid media such as nutrient agar. The agar may be supplemented with various nutrients or antibiotics.

In many cases, an evaluation method is needed to evaluate the efficacy of an antibiotic treatment to kill or inactivate bacterial species. A thin agar layer is needed to isolate targeted bacterial species to observe if they can still multiply after treatment. This is sometimes referred to as the thin agar layer method. Many select media have been developed to isolate a target microorganism. These selective media contain agents designed to select healthy organisms. Although it is helpful for enumeration, the process can be time-consuming.

In this study, we coated a monolayer film of 3-mercaptopropanyl-N-hydroxysuccinimide ester on the surface of the gold-coated SH-SAW biosensor. We saw the concentration dependence in the recorded signal of the glycerol solution concentration. To use a 250 MHz SH-SAW sensor and electronic reader combination. To measure the phase shift and amplitude attenuation, the electronic reader uses a burst circuit that allows us to measure the time delay induced by the added mass while minimizing electromagnetic feed-through from the two delay lines interfering with each other from the activation of each IDT. The sensor reader combination is purchased from TST Biomedical Electronics Company Limited and used without modifications, as seen in Figure 1.

#### *2.4. Bacterial Sample Preparation*

Bacterial samples were prepared from a stock solution cultured over 24 hours and then pelleted by centrifuging the solution for 5 minutes at 4000 revolutions-per-minute (RPMs). The LB Broth nutrient media was decanted. The solution was resuspended in 1x PBS solution.

#### *2.5. Fluorescent Sample Preparation*

The fluorescent samples from the resuspended bacterial solution were prepared from a stock solution cultured over 24 hours and then pelleted. The L.B. Broth nutrient media was decanted and resuspended in 1x PBS. The solution was adjusted to have a final concentration of 5  $\mu$ M of the red fluorescent dye SYTO 11. The cells were incubated in the dark (covered with aluminum foil) for 30 minutes in a 1.5 ml centrifuge tube. After the 30-minute incubation period had expired, the cell suspension was centrifuged for 5 minutes at 4000 RPMs

### **3. Results**

#### *3.1. Fluorescent Imaging*

Fluorescent images were recorded using a Zeiss Axioskop 2 Plus, which is equipped with a Teledyne Lumenera INFINITY5-5 microscopy camera. The INFINITY5-5 is a high-quality 5-megapixel monochrome microscope camera optimized for taking fluorescent images. We then pipetted 5  $\mu$ l of the cells previously stained with SYTO 59 onto the sample area of the SH-SAW biosensor. Imaging was performed directly from the surface of the SH-SAW biosensor mounted on the microscope stage.

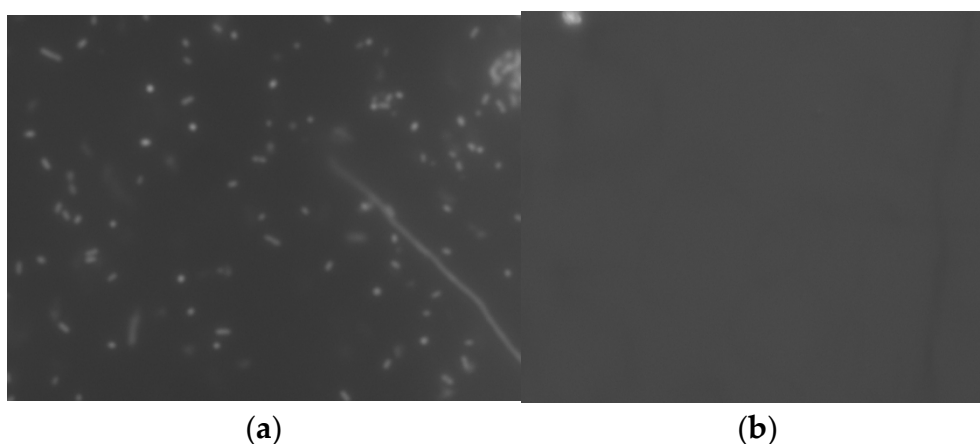


**Figure 3.** Micrograph of the (a) microscope objective imaging the *E. coli K-12* on the biosensor surface (b) fluorescent micrograph of the sensor without *E. coli K-12* cells. Each of the dark objects in the image represents a single *E. coli* cell or a small group of cells. Images taken with 20x 0.50 NA objective.

### 3.2. The effect of the DSP crosslinker

The net effect of coating the SH-SAW biosensor with the 3,3'-Dithiobis (succinimidyl) Propionate (DSP) crosslinker was a modest increase in the phase shift. The addition of DSP was followed by a reduction in a 5mM TCEP solution, forming a layer of 3-mercaptopropanyl-N-hydroxysuccinimide ester on the biosensor's surface. The evidence of the adhesion of the DSP molecule, at least the reduced portion would be the adhesion of *E. coli K-12* cells when no cells are visible in the negative control.

### 3.3. Images of the fluorescent cells on the biosensor

The fluorescent micrographs recorded on the Zeiss Axioskop 2 plus microscope with a trinocular head and fitted with a Lumenera INFINITY5-5 Microscope Camera Teledyne Lumenera, showed brightly fluorescent cells that were easily imaged, as seen in Figure 2 (b). Visible is the yellow excitation light from the filter cubes to excite the red SYTO 59 nucleic acid stain. Visible in the image are groups of viable *E. coli K-12* cells. The cells were imaged with a 20x objective which had a numerical aperture of 0.50, which is why the objects in the image appear to be quite small. We were not able to use a higher magnification of high numerical aperture objectives because they have a much smaller focal length (smaller distance from the objective to the object). The sensor has a 2 mm barrier around the sample reservoir which is longer than the focus length, therefore we are unable to use another of the higher magnification and high numerical aperture objectives. A long working distance objective would be required to focus on the objects in the image.

## 4. Discussion

### 4.1. Sensitivity Measurement

Some of the early work performed to investigate the performance of biosensors used to examine liquid samples using quartz SAW devices was the work reported by Kanazawa and Gordon to explore the frequency shift of bulk wave resonators that were in contact with viscous liquids [32]. That team reported that of a Newtonian fluid, the relative frequency and corresponding phase shift are proportional to the absolute viscosity and density of the liquid [32]. Their model reports the dependence of the frequency shift on the quartz material's elastic modulus and the viscosity-density product of the liquid just about the sensor's surface.

$$\frac{\Delta\varphi}{\varphi_0} = S \sqrt{\frac{\omega\eta\rho}{2}} \quad (2)$$

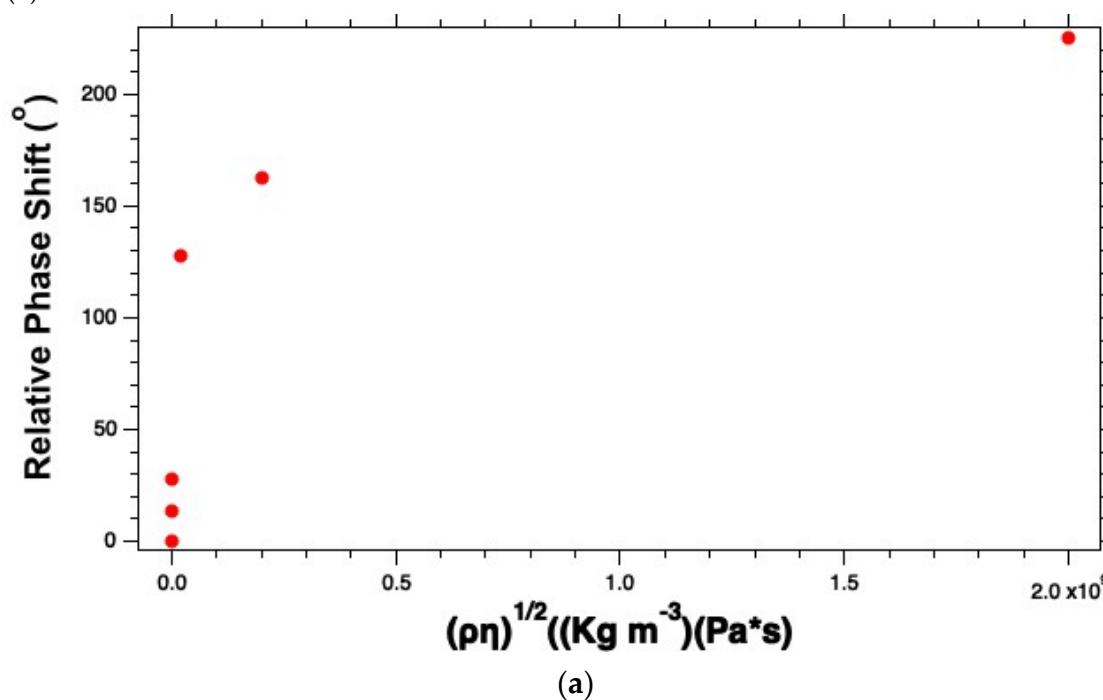
The plot of phase shift versus the square root of the viscosity-density product demonstrates a linear dynamic range in the region from  $2 \times 10^4$  –  $2 \times 10^9$  colony forming unit-per-ml (CFU ml<sup>-1</sup>), as seen

in Figure 4 (a). If we focus on the linear dynamic range, which was over the range from in Figure 4 (b), and employ linear regression, we obtain the sensitivity, which is the absolute value of  $S$  from Eqn. 2,  $|S| = 1.655 \times 10^5 \text{ }^\circ \text{m}^2 \text{ Kg}^{-1}$ . Since the baseline has an average signal of 0.6 and the standard deviation in the baseline signal is 0.04, we can determine the limit of detection for the system, which includes the signal generated by the sensor connected to the reader.

$$LOD = 3.3 * (\text{Standard deviation}) / S \quad (3)$$

**Where  $S$  is the mass sensitivity of the system.** This gives  $S = 1.655 \times 10^5 \text{ }^\circ \text{m}^2 \text{ Kg}^{-1}$ . If we know that the area of the active area of the biosensor is  $1.01 \text{ mm}^2$  or  $1.01 \times 10^{-6} \text{ m}^2$ . In this case, the SH-SAW is a reflector device with a single transducer, and as a result, the wave transverses an area twice as large as the area of the sensor. Therefore, the area of the sensor is  $2 \times (1.01 \times 10^{-6}) \text{ m}^2$  or  $2.02 \times 10^{-6} \text{ m}^2$ . The resulting limit-of-detection (LOD) is  $7.98 \times 10^{-7} \text{ Kg m}^{-2}$  or  $7.98 \times 10^{-10} \text{ g m}^{-2}$  and when adjusted for the area of the sensor traveled by the wave,  $2.02 \times 10^{-6} \text{ m}^2$ , we get an LOD of  $\sim 2.0 \times 10^{-9} \text{ g}$  ( $\sim 2.0 \text{ ng}$ ). This translates to approximately 2,000 *E. coli* K-12 cells since each cell is approximately one picogram.[33]

The frequency response on the SH-SAW device coated with DSP with 1x PBS solutions was recorded and corrected by subtracting the signal of 1x PBS. The sensor's response to an increased liquid is a frequency phase shift proportional to the increase in viscosity. The frequency phase shift results from the impedance of the acoustic wave to the bacterial cells since the effects of the crosslinker and media were removed by subtracting the reference since the phase shift for 1x PBS on a DSP-coated sensor was subtracted. The corrected phase shift is presented in g Figure 4 (a – b) the insertion losses of -28 dB in air, including the propagation loss of the epoxy walls. However, the insertion losses dramatically increase after adding the protein crosslinker. This can be seen in Figure 4 (b).



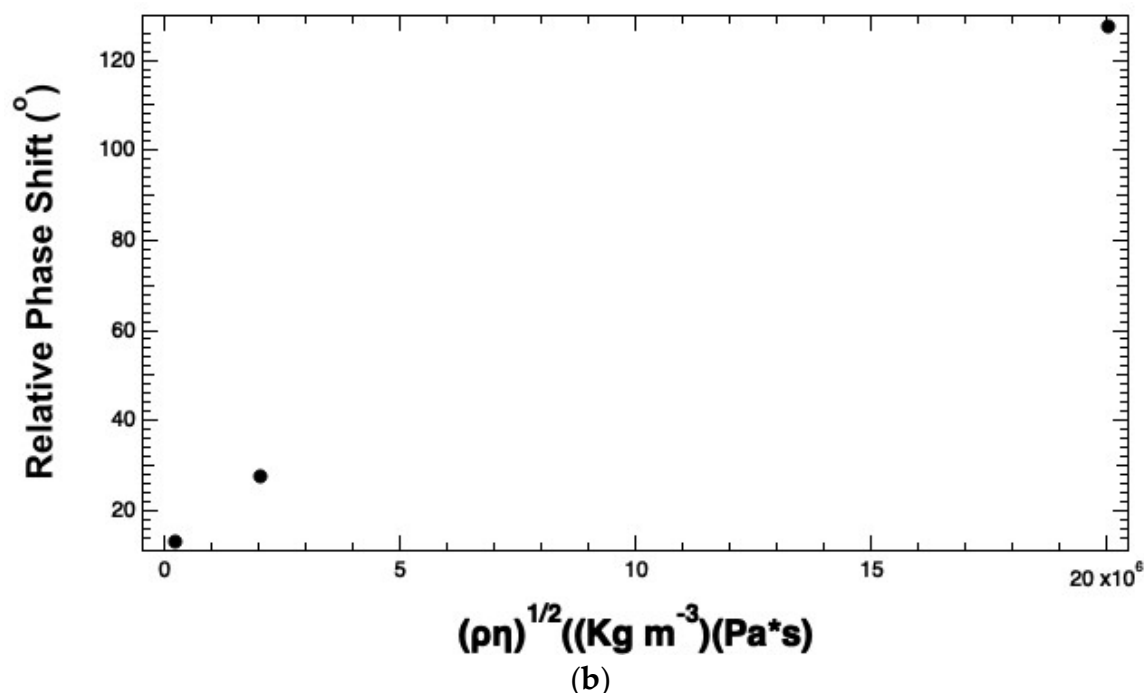


**Figure 4.** Reconstruction of the (a) Phase response curve for the *E. coli* K-12 solutions, and (b) the linear dynamic range by plotting *E. coli* concentrations versus the phase response.

We see that the phase shift plotted versus the density-viscosity product is initially increasing linearly but as the starting concentration of cell increases beyond  $2 \times 10^7$  CFU  $\text{ml}^{-1}$ . This trend deviates drastically as you get to  $2 \times 10^9$  CFU  $\text{ml}^{-1}$ , indicating more of a saturation behavior. We assert that the local viscosity at the surface has become high due to the coating of *E. coli* cells. The linear dynamic range is plotted in Figure 4 (b).

Similarly, we analyzed the insertion to try to understand the effects of the *E. coli* K-12 solution on the insertion loss. There we see similar behaviors. The curves start linear and then appear more like a saturation curve as the starting cell densities exceed  $2 \times 10^7$  CFU  $\text{ml}^{-1}$ . As the *E. coli* K-12 concentrations get closer to  $2 \times 10^9$  CFU  $\text{ml}^{-1}$  the curve starts to look more like a saturation curve. Like the phase versus viscosity-density product, the insertion loss versus the viscosity-density product curve is likely a manifestation of an exceptionally high local viscosity that attenuates the propagating acoustic wave. We suggest not using the instrument in the region of the curve where the curve deviates from linearity. To ensure that this is the case, we recommend diluting the sample if needed to ensure that you stay in the linear dynamic range. This also ensures the accuracy of the results you calculate.

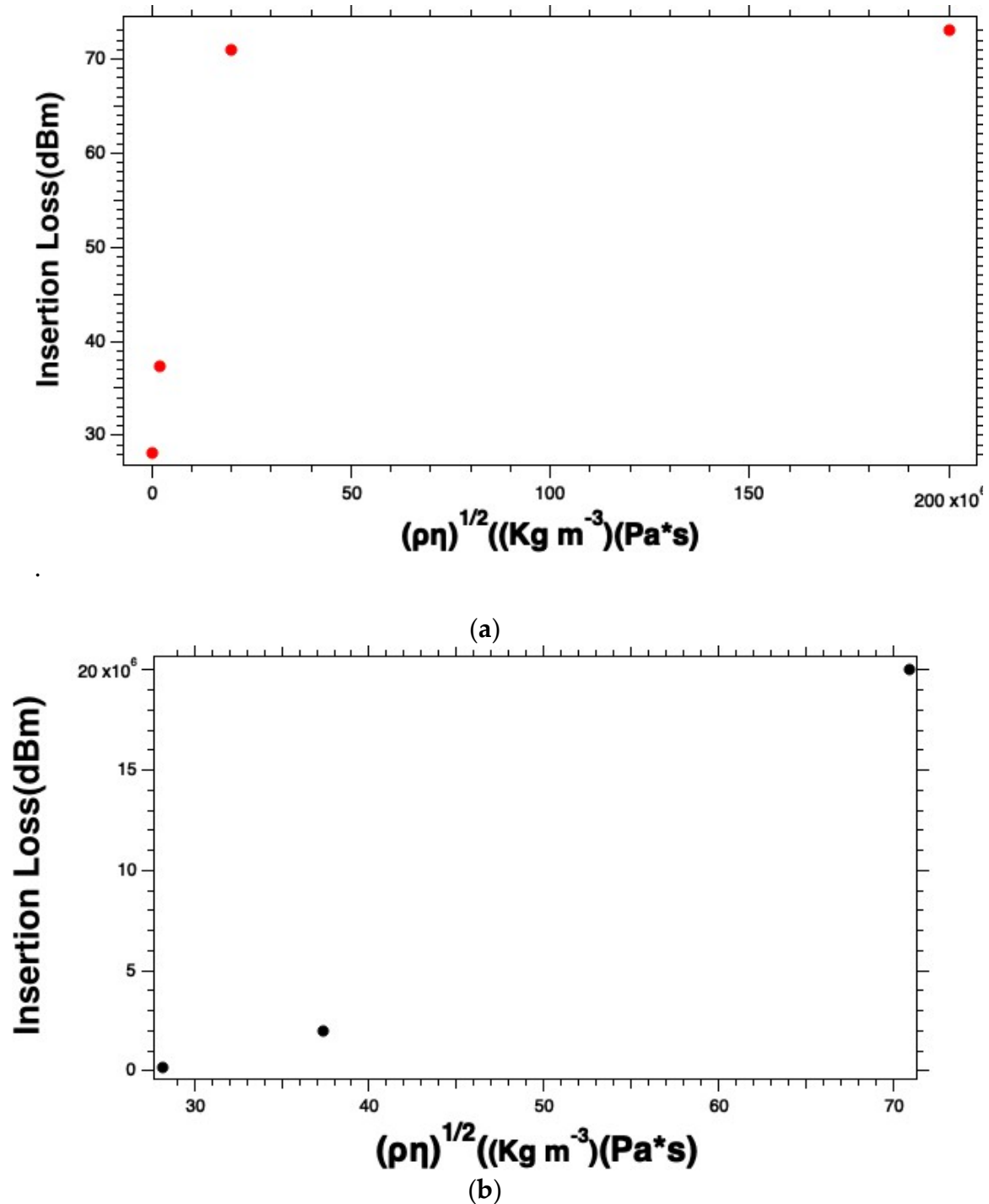


**Figure 5.** Measured insertion losses for (a) the *E. coli* K-12 solutions and (b) the linear dynamic range as a function of starting cell concentrations.

#### 4.2. Characteristics of the Sensor for Bacterial Solutions to the Sensors

To collect our reading, 5  $\mu\text{l}$  of distilled water and record the signal over a 90-second time. Next, we added 5  $\mu\text{l}$  samples of the *E. coli* K-12 solution to the sample well, and the solution was allowed to incubate for 30 minutes at room temperature under similar humidity and environmental conditions. The sensor signal was read and recorded via the electronic reader over the same 90-second period. The curve in Figure 4 (a - b) was generated from plotting the sensor responses to different bacterial concentrations in 1x PBS solution. The responses of the glycerol solutions were expected to be smaller than the signal from the uncoated sensor due to some dampening introduced by the agar coating. However, the signal was still strong enough to measure the viscosity changes

due to adding Glycerol versus air or water. The insertion losses for the uncoated sensor with 1x PBS gave an average of  $27.851 \pm 0.232$  dBm. This value was subtraction as seen in Figure 5 (a - b) for the insertion losses of the biosensor responses *E. coli* K-12 cell solutions. Adding a layer of DSP increased the average insertion losses by only 0.4 dBm, however, the insertion losses on this SH-SAW biosensor are inherently high and range from approximately 28 - 76.5 dBm.

## 5. Conclusions

This report presented data demonstrating the successful analysis of *E. coli* solutions on a DSP-coated SH-SAW that can analyze as little as a  $2 \times 10^5$  CFU per ml *E. coli* K-12 solution. While our study only considered  $2 \times 10^5 - 2 \times 10^9$  CFU ml<sup>-1</sup>, with the linear dynamic range only being in the  $2 \times 10^4 - 2 \times 10^9$  CFU ml<sup>-1</sup> range, lower cell concentrations may be possible by optimizing the crosslinker concentrations and incubation times. However, there is a practical limit. The signal cannot go below the baseline signal. Since the lowest signal measured was  $13.1 \pm 4.8^\circ$ , the practical limit is to measure down to  $4.8^\circ$ . Below this value, you are in an uncertain region. However, this may allow us to go down another order of magnitude to  $2 \times 10^4$ . The net result is that we would be able to down to only 200 cells on the sensor. This is approximately the limit of quantification that we reported previously.<sup>10</sup> We stated that a 50% increase in the signal would constitute a failed test, this would reflect a change of approximately  $6.6^\circ$  which is a number slightly higher than the standard deviation of  $4.8^\circ$ . Therefore, a 50% increase in the phase shift makes sense as the indicator for a confirmed failed test.

We introduced the concept of using an SH-SAW biosensor to demonstrate sterility testing. The sensor response was immediate and steady after introduction to the reader following the 30-minute incubation period. Our results suggest that as little as 2,000 bacterial cells should be easily measured on the DSP-coated sensors. The results suggest bacterial species should be easily captured on the 3-mercaptopropionyl-N-hydroxysuccinimide ester surface of the biosensors. The sensor had very high insertion losses, which is generally concerning. Adding the monolayer of DSP only increased the average insertion losses by only 0.4 dBm, however, the insertion losses on this SH-SAW biosensor ranged from 28 dBm with only 1x PBS - 76.5 dBm with  $2 \times 10^9$  CFU ml<sup>-1</sup> *E. coli* K-12. The sensitivity for our 250 MHz quartz SH-SAW sensors was calculated based on the response from the *E. coli* K-12 solution over the linear dynamic range, which appears to be  $2 \times 10^4 - 2 \times 10^7$  CFU per ml and has a sensitivity of  $S = 1.655 \times 10^5 \text{ }^\circ \text{m}^2 \text{ Kg}^{-1}$ . This assumed an average baseline signal was measured to be  $0.6^\circ$  and a standard deviation of  $0.04^\circ$ .

The LOD of the sensors was calculated to be approximately 2 ng which is estimated to be approximately 2,000 *E. coli* K-12 cells. However, the sensitivity of the DSP-coated sensor was approximately the same as an uncoated sensor. The DSP coating increased the insertion loss by about 1%. Interestingly, the insertion over the range of densities increased by 48.6 dBm with an increase of 44.5 dBm over the linear dynamic range. The phase shift over that same range increased by  $225.3^\circ$  and  $127.5^\circ$  over the linear dynamic range. Our DSP-coated sensor was able to accurately measure down to approximately 2,000 *E. coli* K-12 cells at the lowest concentration measured. However, we believe that our biosensor should be able to detect as little as ~200 bacterial cells by measuring one order of magnitude lower concentration. This measurement would be consistent with theoretical assessments of the sensor previously reported but would require optimization of both the DSP layer and the incubation times.

**Data Statement:** Data for these experiments can be provided upon request. Experimental data is stored in the office of the lead Author, Dr. Marlon Thomas.

The Author (s) declares no conflict of interest. The SH-SAW sensors and electronic readers were purchased from TST Biomedical Electronics Co. in Taipei, Taiwan, and we received no funding from them. All data used in this study was independently measured and analyzed by the authors listed at Fisk University. No animal or human subjects were used to collect the data for this report. However, all Fisk University ethical standards were followed in obtaining data for this report.

**Acknowledgments:** The United States National Science Foundation (NSF), grant number 1817282, and the United States Department of Energy (DOE), grant number 620035, provided funding for this work.

## References

- Ning, S.; Chang, H. C.; Fan, K. C.; Hsiao, P. Y.; Feng, C.; Shoemaker, D.; Chen, R. T., A point-of-care biosensor for rapid detection and differentiation of COVID-19 virus (SARS-CoV-2) and influenza virus using subwavelength grating micro-ring resonator. *Appl Phys Rev* **2023**, *10* (2), 021410.
- Thomas, O. A. E. A. F. B. C. I. M., Sensitivity measurements for a 250 MHz quartz shear-horizontal surface acoustic wave biosensor under liquid viscous loading. *AIP Advances* **2023**, *13*.
- Cheng, C. H.; Yatsuda, H.; Goto, M.; Kondoh, J.; Liu, S. H.; Wang, R. Y. L., Application of Shear Horizontal Surface Acoustic Wave (SH-SAW) Immunosensor in Point-of-Care Diagnosis. *Biosensors (Basel)* **2023**, *13* (6).
- Gray, E. R.; Turbe, V.; Lawson, V. E.; Page, R. H.; Cook, Z. C.; Ferns, R. B.; Nastouli, E.; Pillay, D.; Yatsuda, H.; Athey, D.; McKendry, R. A., Ultra-rapid, sensitive and specific digital diagnosis of HIV with a dual-channel SAW biosensor in a pilot clinical study. *NPJ Digit Med* **2018**, *1*, 35.
- Kano, K.; Yatsuda, H.; Kondoh, J., Evaluation of Shear Horizontal Surface Acoustic Wave Biosensors Using "Layer Parameter" Obtained from Sensor Responses during Immunoreaction. *Sensors (Basel)* **2021**, *21* (14).
- Alhabbab, R. Y., Lateral Flow Immunoassays for Detecting Viral Infectious Antigens and Antibodies. *Micromachines (Basel)* **2022**, *13* (11).
- Thomas, M., Analysis of Red Blood Cell Samples using a Handheld Shear-horizontal Surface Acoustic Wave Biosensor. *International Journal of Biomedical and Clinical Analysis* **2023**, *3* (2), 1-12.
- Taylor, J. J.; Jaedicke, K. M.; van de Merwe, R. C.; Bissett, S. M.; Landsdowne, N.; Whall, K. M.; Pickering, K.; Thornton, V.; Lawson, V.; Yatsuda, H.; Kogai, T.; Shah, D.; Athey, D.; Preshaw, P. M., A Prototype Antibody-based Biosensor for Measurement of Salivary MMP-8 in Periodontitis using Surface Acoustic Wave Technology. *Sci Rep* **2019**, *9* (1), 11034.
- Thomas, M. S., Development of Simple and Portable Surface Acoustic Wave Biosensors for Applications in Biology and Medicine. In *Biosignal Processing*, Karakuş, V. A. a. S., Ed. Intechopen: on-line, 2022.
- Ololade Adetula, E. A., Favour Badewole, Collins Ijale and Marlon Thomas, Sensitivity Measurements for a 250 MHz Quartz Shear-horizontal Surface Acoustic Wave Biosensor under Liquid Viscous Loading. *AIP Advances* **2023**, *13*.
- Hsu-Chao Hao, H.-Y. C., Tsung-Pao Wang, and Da-jeng Yao, Detection of Cells Captured with Antigens on SHear Horizontal Surface-Acoustic-Wave Sensors. *Journal of Laboratory Automation* **2013**, *18* (1), 69-76.
- Klauke, T. N.; Gronewold, T. M.; Perpeet, M.; Plattes, S.; Petersen, B., Measurement of porcine haptoglobin in meat juice using surface acoustic wave biosensor technology. *Meat Sci* **2013**, *95* (3), 699-703.
- Chenyun Wang, C. W., Dan Jin, Yi Yu, Fan Yang, Yulin Zhang, Qunfeng Yao, AuNP-Amplified Surface Acoustic Wave Sensor for the Quantification of Exosomes. *ACS Sensors* **2020**, *5*, 362-369.
- Onrrur Tigli, L. B., cynthia chaterjee, Mona Zaghoul and Patricia Berg In *Surface Acoustic Wave Based Biosensor in CMOS for Cancer Biomarker Detection*, IEEE Sensors 2008 Conference, Lecce, Italy, IEEE: Lecce, Italy, 2008.
- Youn-Suk Choi, J. P. D., Hun Joo Lee, Soo Suk Lee, Joonhyung Lee, Yeol Ho Lee, Sang Kyu Kim, Jung Nam Lee, Kyung Yeon Han and Jae Chan Park In *A Fully-automated Surface Acoustic Wave Immunosensing System for the Detection of Cardiac Markers in Whole Blood*, 15th International Conference on Miniaturized Systems for Chemistry and Life Sciences, Seattle, Washington, Landers, J., Ed. Curran Associates, Inc. ( Apr 2012 ): Seattle, Washington, 2011; p 2118.
- Bisoffi, M.; Severns, V.; Branch, D. W.; Edwards, T. L.; Larson, R. S., Rapid detection of human immunodeficiency virus types 1 and 2 by use of an improved piezoelectric biosensor. *J Clin Microbiol* **2013**, *51* (6), 1685-91.
- Turbe, V.; Gray, E. R.; Lawson, V. E.; Nastouli, E.; Brookes, J. C.; Weiss, R. A.; Pillay, D.; Emery, V. C.; Verrips, C. T.; Yatsuda, H.; Athey, D.; McKendry, R. A., Towards an ultra-rapid smartphone-connected test for infectious diseases. *Sci Rep* **2017**, *7* (1), 11971.
- Abeyawardhane, D. L.; Godoy-Ruiz, R.; Adipietro, K. A.; Varney, K. M.; Rustandi, R. R.; Pozharski, E.; Weber, D. J., The Importance of Therapeutically Targeting the Binary Toxin from *Clostridioides difficile*. *Int J Mol Sci* **2021**, *22* (6).
- Berkenpas, E.; Millard, P.; Pereira da Cunha, M., Detection of Escherichia coli O157:H7 with langasite pure shear horizontal surface acoustic wave sensors. *Biosens Bioelectron* **2006**, *21* (12), 2255-62.
- Thomas, M., Development of Simple and Portable Surface Acoustic Wave Biosensors for Applications in Biology and Medicine. In *Biosignal Processing*, Karakuş, V. A. a. S., Ed. IntechOpen: On-line, 2022; Vol. 1.
- Yatsuda, H., Design techniques for SAW filters using slanted finger interdigital transducers. *IEEE Trans Ultrason Ferroelectr Freq Control* **1997**, *44* (2), 453-9.
- Yatsuda, H., Design technique for nonlinear phase SAW filters using slanted finger interdigital transducers. *IEEE Trans Ultrason Ferroelectr Freq Control* **1998**, *45* (1), 41-7.
- Yatsuda, H.; Yamanouchi, K., Automatic computer-aided design of SAW filters using slanted finger interdigital transducers. *IEEE Trans Ultrason Ferroelectr Freq Control* **2000**, *47* (1), 140-7.

24. Hussain, A.; Zaman, G.; Satti, L.; Ikram, A.; Gardezi, A. H.; Khadim, M. T., Evaluation of Thin Layer Agar 7H11 for Direct Susceptibility Testing of Mycobacterium Tuberculosis Complex against Second Line Anti Tuberculosis Drugs on Smear Positive Specimens. *J Coll Physicians Surg Pak* **2019**, *29* (6), 520-523.
25. Ardizzoni, E.; Mulders, W.; Kotrikadze, T.; Aspindzelashvili, R.; Goginashvili, L.; Pangtey, H.; Varaine, F.; Bastard, M.; Rigouts, L.; de Jong, B. C., The thin-layer agar method for direct phenotypic detection of multi- and extensively drug-resistant tuberculosis. *Int J Tuberc Lung Dis* **2015**, *19* (12), 1547-52.
26. Martin, A.; Paasch, F.; Von Groll, A.; Fissette, K.; Almeida, P.; Varaine, F.; Portaels, F.; Palomino, J. C., Thin-layer agar for detection of resistance to rifampicin, ofloxacin and kanamycin in Mycobacterium tuberculosis isolates. *Int J Tuberc Lung Dis* **2009**, *13* (10), 1301-4.
27. Martin, A.; Fissette, K.; Varaine, F.; Portaels, F.; Palomino, J. C., Thin layer agar compared to BACTEC MGIT 960 for early detection of Mycobacterium tuberculosis. *J Microbiol Methods* **2009**, *78* (1), 107-8.
28. Kang, D. H.; Fung, D. Y., Thin agar layer method for recovery of heat-injured *Listeria monocytogenes*. *J Food Prot* **1999**, *62* (11), 1346-9.
29. Hill, D. R., Thin agar film for enhanced fungal growth and microscopic viewing in a new sealable fungal culture case. *J Clin Microbiol* **1996**, *34* (9), 2140-2.
30. Peng, Y. C.; Cheng, C. H.; Yatsuda, H.; Liu, S. H.; Liu, S. J.; Kogai, T.; Kuo, C. Y.; Wang, R. Y. L., A Novel Rapid Test to Detect Anti-SARS-CoV-2 N Protein IgG Based on Shear Horizontal Surface Acoustic Wave (SH-SAW). *Diagnostics (Basel)* **2021**, *11* (10).
31. Darren W. Branch, T. L. E., Dale Huber, and Susan M. Brozik *Shear Horizontal Surface Acoustic Wave Microsensor for Class A Viral and Bacterial Detection*; Sandia National Laboratories: Issued by Sandia National Laboratories, operated for the United States Department of Energy by Sandia Corporation., 2008.
32. K. Kanazawa, J. G. I., The Oscillation Frequency of a Quartz Resonator in Contact with a Liquid. *Anal Chim Acta* **1985**, *175*, 99-105.
33. Phillips, R.; Kondev, J.; Theriot, J., *Physical biology of the cell*. Garland Science: New York, 2009; p xxiv, 807 p.

**Disclaimer/Publisher's Note:** The statements, opinions and data contained in all publications are solely those of the individual author(s) and contributor(s) and not of MDPI and/or the editor(s). MDPI and/or the editor(s) disclaim responsibility for any injury to people or property resulting from any ideas, methods, instructions or products referred to in the content.